

Oxide and carbonate surfaces as environmental interfaces: the importance of water in surface composition and surface reactivity

Hind A. Al-Abadleh, Hashim A. Al-Hosney, Vicki H. Grassian*

Department of Chemistry and the Center for Global and Regional Environmental Research, University of Iowa, Iowa City, IA 52242, USA

Available online 11 November 2004

Abstract

Environmental molecular surface science is an important and expanding area of current research. Here we give a brief review of the chemical nature of two representative oxide and carbonate surfaces, MgO(100) and CaCO₃(104), under ambient conditions of temperature and relative humidity. Studies using a variety of spectroscopic techniques have shown that water readily dissociates on these surfaces under ambient conditions leaving a surface truncated with hydroxyl groups. For MgO, the surface stoichiometry is best represented as Mg(OH)₂ whereas for CaCO₃, it is Ca(OH)(CO₃H). Water readily adsorbs on these hydroxylated surfaces. This adsorbed water layer plays an important role in the reactivity of MgO(100) and CaCO₃(104) under ambient conditions. The adsorption of nitric acid, a trace gas found in the troposphere, on MgO(100) and CaCO₃(104) surfaces under dry (<1% RH) and wet conditions (20–25% RH) demonstrates this point. Adsorption at higher relative humidity results in the formation of nitrate thin films that are on the order of 10–100 layers thick. Water uptake on these thin nitrate films results in several phase transitions as a function of relative humidity. Thus the results presented here are meant to demonstrate the importance of adsorbed water in the surface composition and surface reactivity of oxide and carbonate surfaces.

© 2004 Elsevier B.V. All rights reserved.

Keywords: Magnesium oxide; Calcium carbonate; Environmental interfaces; Water adsorption; Nitric acid adsorption

1. Introduction

It is clear that as environmental problems and concerns increase there will be a need to better understand environmental processes on a molecular level. Oxide and carbonate surfaces are important environmental interfaces as they play a role in several environmental processes including environmental catalysis and remediation, heterogeneous atmospheric chemistry and aqueous geochemistry. Fig. 1 shows a cartoon depicting the various ways oxide and carbonate surfaces are involved in environmental processes as catalysts and adsorbents in industry and automobiles and as natural interfaces in air, water and soil.

Since reactions of environmental importance most often occur under ambient conditions of atmospheric pressure and temperature or in the aqueous phase, it is important to understand the nature of the oxide interface under these conditions. Adsorption of molecules such as H₂O and CO₂ will change

the stability of these surfaces [1]. It is therefore important to account for the effect of adsorption of atmospheric gases including H₂O and CO₂ on the overall stability of oxide surfaces under ambient conditions.

In the natural environment, the relative humidity is between 20 and 90% RH ($RH = p/p_o \times 100$, where p_o = saturated vapor pressure of liquid water). This means that at 295 K, there is somewhere between 5 and 20 Torr water vapor pressure in the atmosphere at all times. In the case of metal oxide surfaces, dissociation of water molecules at the interface is energetically favored by the fact that hydroxylated surfaces are in general more stable than metal-terminated surfaces under ambient conditions [2]. Hydroxylation occurs in part to complete the coordination environment of the metal and oxygen ions especially at defect sites such as oxygen vacancies and steps. Carbonate surfaces have not been as well studied. However, as discussed in more detail in this review, it has been shown that these surfaces are also terminated with OH groups.

Since the surfaces of oxides and carbonates under ambient conditions are terminated with hydroxyl groups, they

* Corresponding author. Tel.: +1 319 335 1392; fax: +1 319 353 1115.
E-mail address: vicki-grassian@uiowa.edu (V.H. Grassian).

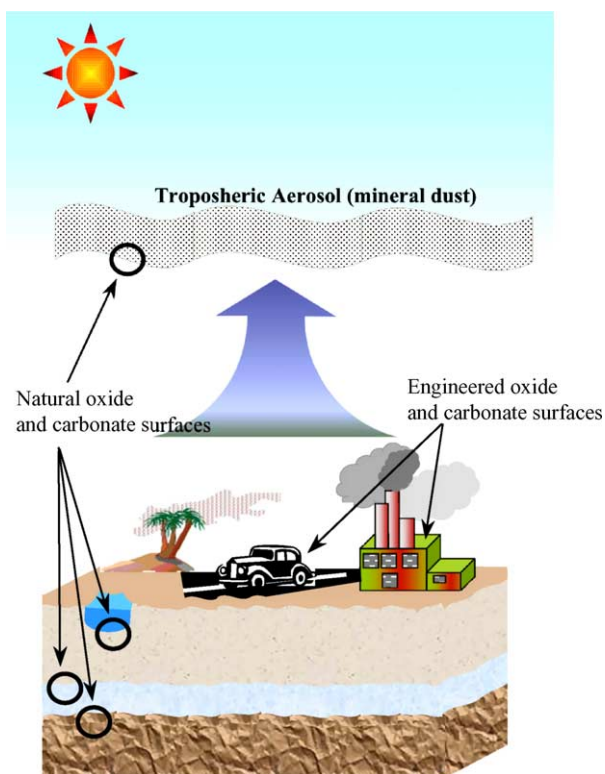


Fig. 1. A cartoon depicting the various ways natural and engineered oxide and carbonate surfaces are involved in environmental processes including catalysis and remediation, heterogeneous atmospheric chemistry, and aqueous geochemistry. Adapted from H.A. Al-Abadleh, V.H. Grassian, Oxide surfaces as environmental interfaces, *Surf. Sci. Rep.* 52 (2003) 63–162. Copyright (2003), with permission from Elsevier.

can readily adsorb water [3,4]. The presence of adsorbed water will play a role in the reactivity of these surfaces [5–7]. Thus, studies undertaken to better understand the chemistry of environmental interfaces must employ a combination of surface-sensitive techniques. Importantly, some of these techniques need to operate under ambient conditions of pressure and temperature as well as those that operate in an ultra-high vacuum (UHV) environment.

In this paper, we present a brief review of experiments that give some insight into the chemical nature of two representative oxide and carbonate surfaces, MgO and CaCO₃ respectively, under environmental conditions. Much of the discussion is on well-defined, single crystal surfaces, MgO(1 0 0) and CaCO₃(1 0 4), however, powdered samples are also discussed. Magnesium oxide is an ideal model for ionic metal oxides because it forms the rock salt structure and has a relatively simple electronic structure that can be modeled using ab initio theories [8,9]. For rock salt crystals, the most stable surface face is the 1 0 0 plane [2]. In the case of calcium carbonate, there are two stable polymorphs at ambient pressure and temperature, calcite and aragonite [10]. The bulk crystal structure of calcite is rhombohedral whereas for aragonite, it is orthorhombic. Most studies to date have focused on different calcite surface planes. For calcite, the

(1 0 4), (1 0 1) and the (1 1 0) surfaces have been theoretically modeled, with the (1 0 4) surface being the lowest energy surface plane [11].

The surface chemistry of nitric acid on MgO and CaCO₃ surfaces under “dry” conditions (<1% RH) and “wet” conditions (~25% RH) is presented as an example of the importance of water in the reactivity of MgO and CaCO₃. The resultant films of magnesium and calcium nitrate that form from reaction of HNO₃ on MgO(1 0 0) and CaCO₃(1 0 4), respectively undergo phase transitions as a function of relative humidity. The role of adsorbed water in the uptake of nitric acid on MgO and CaCO₃ and phase transitions in the resultant salt films are discussed.

2. Composition of oxide and carbonate environmental interfaces: MgO and CaCO₃

2.1. Magnesium oxide

The 1 0 0 surface, shown in Fig. 2, is the most stable surface of magnesium oxide and other oxides with the rock salt structure [2]. Well-defined thin films of MgO(1 0 0) can be grown on various substrates at low temperature by evaporating Mg in a background of oxygen [12–14]. This is of great interest as MgO is used in catalysis as an oxide support [15].

Hydroxylation of MgO surfaces and the structure and dynamics of the water/MgO interface have been extensively studied both by theory [16–22] and experiment [8,9,23–33].

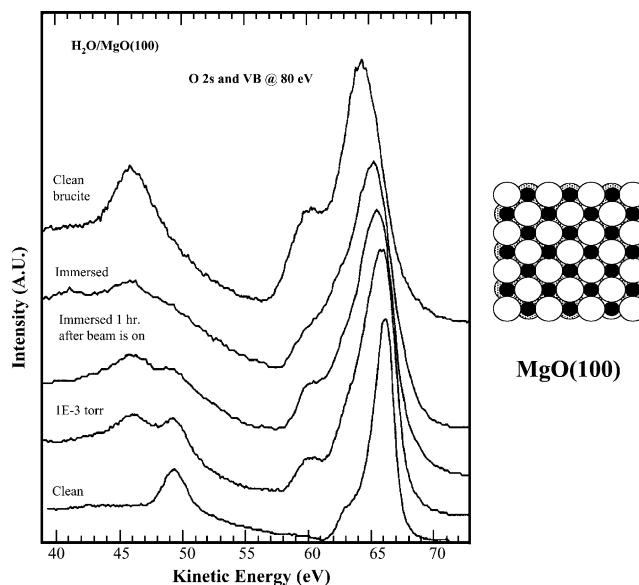


Fig. 2. Bulk-terminated surface structures of MgO(1 0 0) and photoemission spectra of the O 2s/valence band spectra are shown for clean MgO(1 0 0), water-dosed [$p(\text{H}_2\text{O})=1 \times 10^{-3}$ Torr for 3 min] MgO(1 0 0), and water-immersed MgO(1 0 0). For reference, a clean brucite (Mg(OH)₂) surface is also shown. Adapted from P. Liu, T. Kendelewicz, G.E. Brown Jr., G.A. Parks, Reaction of water with MgO(1 0 0) surfaces. Part I. Synchrotron X-ray photoemission studies of low-defect surfaces, *Surf. Sci.* 412–413 (1998) 287–314. Copyright (1998), with permission from Elsevier.

Most calculations done at different levels of theory for the water/MgO system have found that for the most part water reversibly physisorbs on defect-free MgO surface, and that hydroxylation occurs only at defect sites. Other theoretical studies found that dissociation of water molecules on flat MgO surfaces can occur through a mechanism stabilized by hydrogen bonding [16,20,21,24,34]. Most experimental studies of water adsorption on MgO surfaces are done under UHV conditions and results vary depending on the temperature, pressure, and crystal cleavage procedure. In general, results from UHV studies range from molecular to dissociative adsorption of water at low water exposures and multilayer water formation at high water exposures. Liu et al. obtained spectra of the O 2s/valence band using photoelectron spectroscopy of clean, water vapor exposed [$p(\text{H}_2\text{O}) = 1 \times 10^{-3}$ Torr for 3 min], water-immersed MgO(1 0 0) surfaces at 300 K, and of brucite ($\text{Mg}(\text{OH})_2$) for Ref. [8]. These spectra are shown in Fig. 2. The vacuum cleaved, “low defect” MgO(1 0 0) surface is found to adsorb water by first forming hydroxyl groups. Defects such as steps, corners and vacancy sites are found to hydroxylate at water pressures far less than what is required to hydroxylate terraces [9]. After complete hydroxylation of the surface, it is found to reconstruct to an overlayer of stoichiometry $\text{Mg}(\text{OH})_2$.

Molecularly adsorbed water molecules can then interact with $\text{Mg}(\text{OH})_2$ terminated surfaces via hydrogen-bonding. Foster et al. studied water adsorption on single crystal surfaces of MgO(1 0 0) cleaved in a N_2 atmosphere using transmission Fourier transform infrared (FTIR) spectroscopy at 296 K in the presence of 0.2–21 Torr H_2O vapor pressure corresponding to 1–99% relative humidity (RH) [33]. Based on the shape of the adsorption isotherm (see Fig. 3a) and the invariant nature of the water absorption band as a function of coverage, Foster et al. concluded that water grows in three-dimensional patches on the surface. Interestingly, the adsorption isotherm also showed evidence for hysteresis in the adsorption/desorption curves.

Based on the results of all of these studies, it can be concluded that the 1 0 0 surface plane of MgO will be coated with more than one layer of molecularly adsorbed water at water vapor pressures above ~ 1 Torr ($\sim 5\%$ RH) and that underlying this adsorbed water layer is a surface best represented as $\text{Mg}(\text{OH})_2$.

2.2. Calcium carbonate

Water adsorption on calcite in ambient gas-phase environments and the dissolution of calcite in aqueous environments have been the focus of several studies [35–42]. Studies done to understand the fundamental aspects of macroscopic processes such as calcite dissolution have utilized single crystal surfaces and most often the lowest energy plane, the (1 0 4) surface. Atomic force microscopy (AFM) has been a particularly useful tool in these studies. Results of high resolution AFM images at the atomic level of freshly cleaved $\text{CaCO}_3(1 0 4)$ surfaces reveal that exposure to humid air

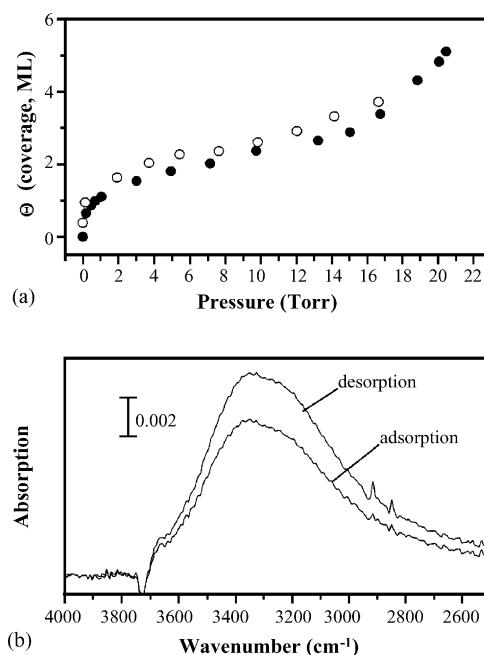


Fig. 3. (a) Adsorption isotherm for water on MgO(1 0 0) ($T = 298$ K) measured for ascending and descending pressures as represented by closed and open circles, respectively. An example of the absorption spectra of water for an adsorption and desorption cycle is shown in (b). Adapted from M. Foster, M. Rurse, D. Passno, An FTIR study of water thin films on magnesium oxide, Surf. Sci. 502–503 (2002) 102–108. Copyright (2002), with permission from Elsevier.

or liquid water results in the formation of etch pits tens of nanometers in width after reaching equilibrium [35–38]. Such observations have been assigned to the formation of an adsorbed hydration layer where water is chemisorbed to dangling bonds of the bulk-terminated surface generating stable adsorbed hydrolysis products, namely $\text{S}\cdot\text{CO}_3\text{H}$ and $\text{S}\cdot\text{CaOH}$, where S is the surface.

In addition to AFM, other surface analysis methods have been applied to the understanding of $\text{CaCO}_3(1 0 4)$. Stipp has recently summarized what is known about the calcite surface from several techniques including X-ray photoelectron spectroscopy (XPS), low energy electron diffraction (LEED), and time-of-flight secondary ion mass spectrometry (TOF-SIMS) [38]. A side-on view of the structure of a bulk terminated $\text{CaCO}_3(1 0 4)$ surface is shown in Fig. 4 along with the XPS spectra of the O 1s and C 1s peaks of a $\text{CaCO}_3(1 0 4)$ surface cleaved in air. There is evidence for surface CO_3H and OH in the XPS spectra. TOF-SIMS chemical maps of a sample cleaved in air show high O and H signals suggesting an increase in the surface concentration of OH species from exposure to H_2O in the atmosphere.

The interaction of water with $\text{CaCO}_3(1 0 4)$ has been theoretically modeled [11,39–41]. A molecular modeling study of different modes of adsorption of a single water molecule on the (1 0 4) surface plane was carried out by minimizing the interaction energy [39]. It was found that replacement of a carbonate ion by a surface hydroxyl and bicarbonate ion is energetically more favorable than replacement by two

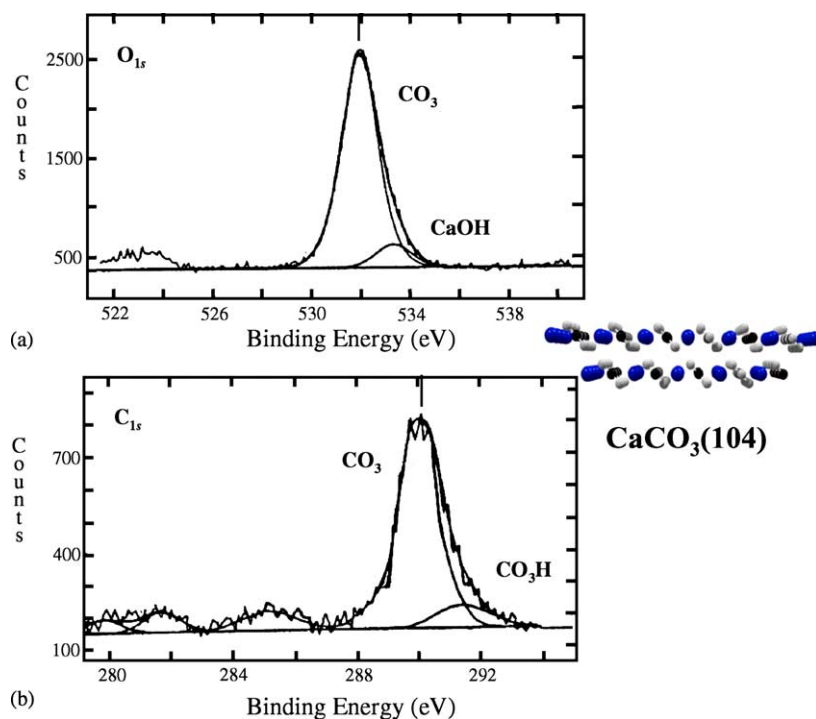


Fig. 4. X-ray photoelectron spectroscopy of a $\text{CaCO}_3(104)$ sample exposed to water vapor from the ambient environment; (a) O 1s and (b) C 1s regions. Surface species OH and CO_3H seen in the spectra are consisted with water dissociation on the surface. Adapted from S.L.S. Stipp, Toward a conceptual model of the calcite surface: hydration, hydrolysis and surface potential, *Geochim. Cosmochim. Acta* 63 (1999) 3121–3131. Copyright (1999), with permission from Elsevier. A side-on-view of bulk-terminated $\text{CaCO}_3(104)$ is also shown.

hydroxyl ions. deLeeuw and Parker employed atomistic simulation techniques for investigating the molecular adsorption of water on the low-index surfaces of different polymorphs of calcium carbonate [11]. The main finding of the calculations was that all surfaces investigated tend to be hydrated to full monolayer coverage and calculated hydration energies were in good agreement with experimental values.

Water adsorption on CaCO_3 particles at $T = 296$ K has recently been investigated with Attenuated Total Reflection ATR-FTIR spectroscopy [43]. The ATR-FTIR spectra of CaCO_3 particles recorded as a function of relative humidity are shown in Fig. 5. Intense absorption bands labeled in the spectra at 878 and 1434 cm^{-1} are assigned to the ν_2 and ν_3 modes, respectively, of bulk CO_3^{2-} . As the relative humidity increases, absorption bands in the water bending and stretching mode regions near 1646 and 3372 cm^{-1} , respectively, begin to grow in. Interestingly, in the spectra recorded below $\sim 55\%$ RH, the O–H stretching band has distinct structure compared to the spectra recorded at higher relative humidity and the full-width-half-maxima of the water bending mode below $\sim 55\%$ RH is narrower than it is at higher relative humidity. These differences in spectral features below $\sim 55\%$ RH compared to the spectra above $\sim 55\%$ RH suggest that water adsorbs first in a two-dimensional network and then above $\sim 55\%$ RH, multilayers begin to form. This is similar behavior to what has been found for water adsorption on several other mineral surfaces including mica and BaF_2 [44,45].

Thus it is clear that calcite surfaces are terminated with OH groups representing surface species of OH and CO_3H that persist even under UHV conditions [38,42]. Furthermore, in the presence of water vapor between 10–90% RH, there is molecularly adsorbed water on top of the OH and CO_3H layer. Therefore, the surface chemistry of calcium carbonate under ambient conditions will depend on the chemistry of the

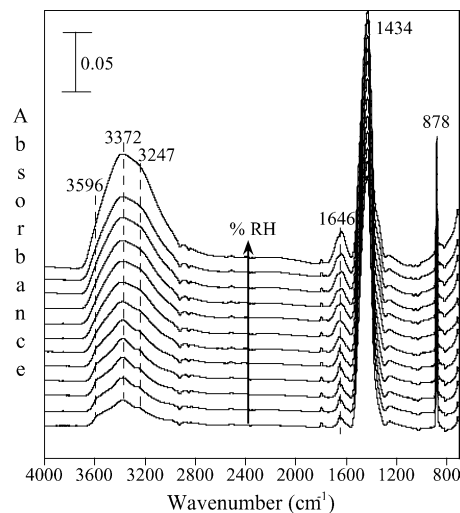


Fig. 5. ATR-FTIR spectroscopy of CaCO_3 particles at $T = 296$ K, as a function of relative humidity; spectra were recorded at 20.2, 25.4, 35.4, 41.6, 45.4, 50.1, 55.8, 60.1, 65.6, 70.7, 77.3, 81.5 and 95.3% RH.

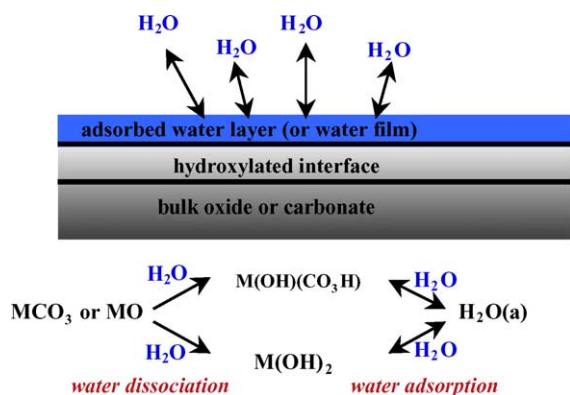


Fig. 6. Pictorial cartoon of oxide and carbonate environmental interfaces. Water dissociation and water adsorption change the chemical composition of the surface from that of the bulk. Dissociative adsorption of water gives rise to a hydroxylated surface that is stable even under UHV conditions. In the presence of water vapor, water molecularly adsorbs on the surface to form a thin water film. The reactivity of these two interfaces, hydroxylated surface and adsorbed water layer, will control the reaction chemistry of oxide and carbonate surfaces under environmental conditions.

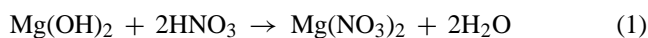
interface defined by the hydroxylated surface and the water thin film adsorbed on that layer.

Fig. 6 shows a pictorial cartoon of the oxide and carbonate interfaces, represented as MO and MCO_3 , respectively, after being exposed to ambient conditions. Under dry conditions (<1% RH), OH groups persist even under UHV conditions from the irreversible dissociation of water on the surface whereas at higher relative humidity molecularly adsorbed water in equilibrium with water vapor covers the surface. The reactivity of these interfaces, hydroxylated surface and water adsorbed on the hydroxylated surface, with nitric acid vapor is discussed in the next two sections.

3. Nitric acid adsorption on oxide and carbonate environmental interfaces

3.1. Magnesium oxide: reaction under dry conditions

FTIR studies of reaction of nitric acid vapor under dry conditions (<1% RH), i.e., in the absence of any appreciable amounts of molecularly adsorbed water on $\text{MgO}(1\ 0\ 0)$, has shown that $\text{Mg}(\text{NO}_3)_2$ forms on the surface [46]. Given the above discussion, this reaction most likely occurs according to reaction (1)

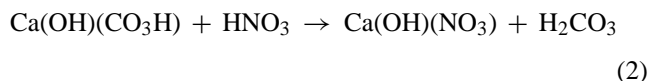


The nitrate layer may form via a two-step mechanism involving the consecutive replacement of each of the OH groups from the surface. Quantitative analysis of the FTIR data, show that the surface coverage of nitrate ions, $S_{\text{NO}_3} = 2.3 \pm 0.1 \times 10^{15}$ ions cm^{-2} for nitric acid reaction with MgO under dry conditions. This coverage is consistent with the formation of one monolayer of $\text{Mg}(\text{NO}_3)_2$. Although water forms in the reaction according to (1), the reaction ap-

pears to be limited to one monolayer of $\text{Mg}(\text{NO}_3)_2$ under dry reaction conditions (<1% RH).

3.2. Calcium carbonate: reaction under dry conditions

Nitric acid uptake on calcium carbonate particles under dry conditions has been reported by Goodman et al. [47]. Similar to reaction of nitric acid on MgO , the reaction is limited to the surface of the calcium carbonate particles. There is some evidence for the formation of carbonic acid, H_2CO_3 , in these reactions and is thought to occur according to reaction (2) [43],



Carbonic acid is an intermediate in the surface chemistry of carbonate minerals in aqueous solution, although in solution it quickly dissociates into CO_2 and H_2O . The adsorbed carbonic acid also dissociates readily in the presence of adsorbed water [48].

Enhanced uptake of nitric acid on oxide and carbonate environmental interfaces under wet conditions and phase transitions in thin $\text{Mg}(\text{NO}_3)_2$ and $\text{Ca}(\text{NO}_3)_2$ films as a function of relative humidity are discussed in the next two sections.

3.3. Magnesium oxide: reaction under wet conditions

Al-Abadleh and Grassian have shown that reaction of nitric acid vapor with $\text{MgO}(1\ 0\ 0)$ under wet conditions, defined as 25% RH, at 298 K is not limited to the surface but underlying layers can react [46]. As discussed in the preceding section, under dry conditions, nitric acid uptake on $\text{MgO}(1\ 0\ 0)$ is limited to the topmost surface layer and saturates at a nitrate coverage of $2.3 \pm 0.1 \times 10^{15}$ ions cm^{-2} to form a single layer of magnesium nitrate. However, in the presence of water vapor at 25% relative humidity (RH), sub-surface layers are found to be reactive and the extent of nitric acid uptake significantly increases. Magnesium nitrate forms on the host MgO without evidence of saturation. The infrared spectra following reaction under three different reaction conditions are shown in Fig. 7. The spectra were recorded under dry conditions (<1% RH). The two spectra labeled 25% RH were done at different pressures of nitric acid, leading to two different final nitrate coverages. The nitrate coverages obtained from these different reactions is determined from the integrated absorption of the nitrate bands near $1400\ \text{cm}^{-1}$. It can be seen that the extent of reaction is much greater in the presence of water vapor and that thin films of magnesium nitrate are estimated to be 10–100 nm thick.

Water uptake on the surface of these thin magnesium nitrate films results in several phase transitions. These phase transitions were probed with infrared spectroscopy as a function of relative humidity. Water adsorption and desorption isotherms on nitrated- $\text{MgO}(1\ 0\ 0)$ surfaces following reaction with nitric acid were measured at 296 K. The transmission

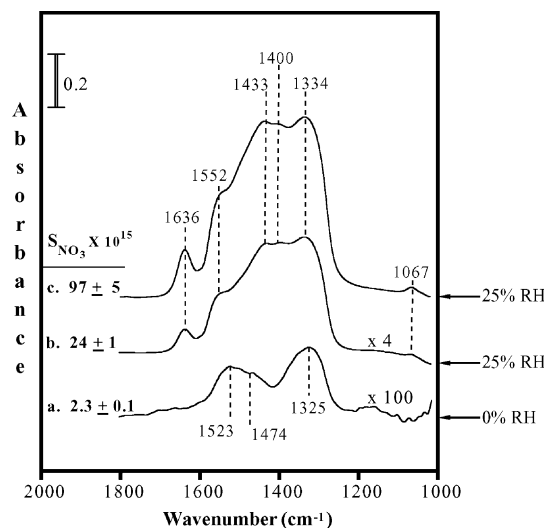


Fig. 7. Transmission FT-IR spectra of MgO(100): (a) following reaction with nitric acid under dry conditions, $S_{\text{NO}_3} = 2.3 \pm 0.1 \times 10^{15}$ ions cm^{-2} ; (b) following reaction under wet conditions (25% RH) giving a surface coverage, $S_{\text{NO}_3} = 2.4 \pm 0.1 \times 10^{16}$ ions cm^{-2} ; and (c) under wet conditions giving a higher surface coverage, $S_{\text{NO}_3} = 9.7 \pm 0.5 \times 10^{16}$ ions cm^{-2} . Adapted with permission from H.A. Al-Abadleh and V.H. Grassian, Phase transitions in magnesium nitrate thin films: a transmission FT-IR study of the deliquescence and efflorescence of nitric acid reacted magnesium oxide interfaces, *J. Phys. Chem. B* 107 (2003) 10829. Copyright (2003) American Chemical Society.

FTIR spectra of water adsorption on MgO(100) that had been reacted with nitric acid are shown in Fig. 8 for the lowest nitrate film coverage. Besides observing an overall increase in intensity in the absorption bands associated with the bending mode, $\delta(\text{H}_2\text{O})$, and the O–H stretching mode, $\nu(\text{OH})$, of ad-

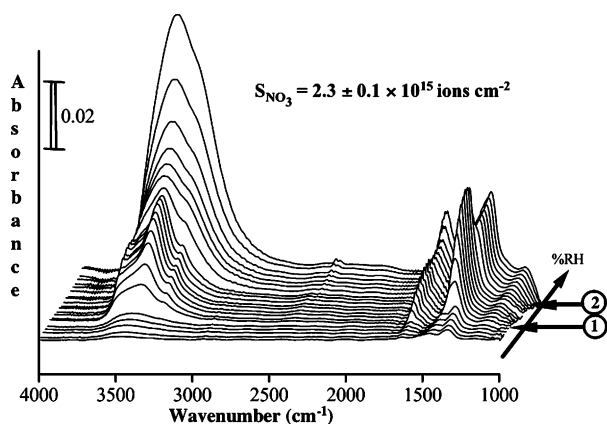


Fig. 8. Transmission FT-IR spectra of water adsorption on MgO(100) reacted previously with HNO_3 under dry conditions at a nitrate coverage of $2.3 \pm 0.1 \times 10^{15}$ ions cm^{-2} . The spectra are recorded as a function of increasing %RH; 0.57, 1.4, 2.3, 3.5, 4.4, 9.2, 14, 19, 24, 28, 33, 38, 43, 47, 52, 57, 62, 66, 76, 84 and 93. Two phase transitions (labeled 1 and 2) are observed as a function of relative humidity. See text for further details. Adapted with permission from H.A. Al-Abadleh and V.H. Grassian, Phase transitions in magnesium nitrate thin films: a transmission FT-IR study of the deliquescence and efflorescence of nitric acid reacted magnesium oxide interfaces, *J. Phys. Chem. B* 107 (2003) 10829. Copyright (2003) American Chemical Society.

sorbed water in the spectral regions extending from 1500 to 1800 cm^{-1} and 2800 to 3800 cm^{-1} , respectively, the spectra show very interesting changes in the nitrate spectral features as a function of increasing water vapor pressure as well. These changes can be correlated to two phase transitions occurring in these films. One transition occurs at low relative humidity, <10% RH, corresponding to the formation of crystalline magnesium nitrate hydrates, $\text{Mg}(\text{NO}_3)_2 \cdot n\text{H}_2\text{O}$, $4 < n < 6$, from an amorphous salt film. The second phase transition occurs between 49 and 55% RH and corresponds to the deliquescence of crystalline $\text{Mg}(\text{NO}_3)_2 \cdot 6\text{H}_2\text{O}$ to an aqueous salt solution. Thinner films deliquesce at $49 \pm 2\%$ RH, whereas thicker nitrate films deliquesce at $54 \pm 2\%$ RH which is within experimental error of the value for pure $\text{Mg}(\text{NO}_3)_2 \cdot 6\text{H}_2\text{O}$ crystals. A hysteresis is seen as a function of decreasing relative humidity, and the transition corresponding to efflorescence, i.e., crystallization as a function of decreasing RH, depends to an even greater extent on the film thickness. Thinner films of magnesium nitrate show no evidence of efflorescence whereas thicker films show efflorescence at $48 \pm 3\%$. A pictorial representation of the phase changes in the thin film as a function of increasing and decreasing relative humidity is shown in Fig. 9.

Al-Abadleh and Grassian also showed that efflorescence (crystallization) as a function of decreasing relative humidity is not observed for the thinnest magnesium nitrate films studied as there may be an absence of nucleation sites on these smooth surfaces [46]. AFM images of nitric acid reacted MgO(100) surfaces showed that the surface roughness increased significantly for the thicker films. The rougher

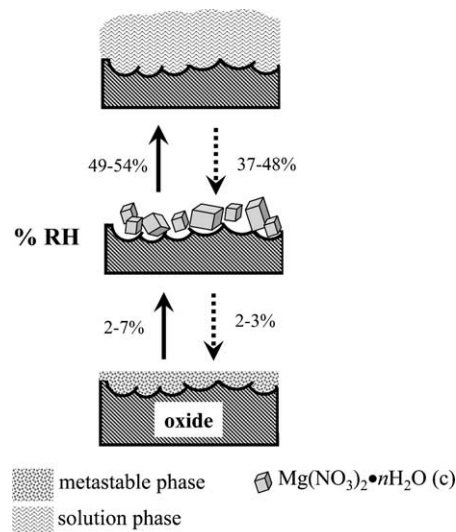


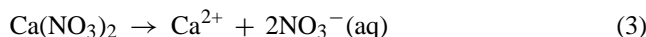
Fig. 9. A schematic diagram showing phase transitions of nitrate films on MgO(100) surfaces as a function of relative humidity at 296 K observed in this study. The solid and dashed arrows are for increasing %RH and decreasing %RH, respectively. See text for further details. Reprinted with permission from H.A. Al-Abadleh and V.H. Grassian, Phase transitions in magnesium nitrate thin films: a transmission FT-IR study of the deliquescence and efflorescence of nitric acid reacted magnesium oxide interfaces, *J. Phys. Chem. B* 107 (2003) 10829. Copyright (2003) American Chemical Society.

surface and the size of the features, on the order of nanometers in dimension, provide nucleation sites for crystallization to occur. These results are significant as they show phase transitions in thin films, tens to hundreds of nanometers thick, have very different behavior than that found in the bulk phase.

3.4. Calcium carbonate: reaction under wet conditions

Al-Abadleh et al. investigated water uptake on thin films of $\text{Ca}(\text{NO}_3)_2$ supported on CaCO_3 [49]. Thin films of calcium nitrate, $\text{Ca}(\text{NO}_3)_2$, were prepared by reaction of $\text{CaCO}_3(1\ 0\ 4)$ with nitric acid vapor (~ 200 m Torr). The reaction was done at room temperature ($T = 296$ K) and under wet conditions (23% RH) in order for films greater than one layer to form. After reaction of calcite with nitric acid vapor, the hygroscopic response of the surface increased significantly.

Unlike magnesium nitrate thin films, only one phase transition is observed for these thin films, the transition from an amorphous nitrate phase to a calcium nitrate solutions according to reaction 3.



This can be readily seen in Fig. 10 which shows the hygroscopic response, measured by the number of water layers taken up by the surface, as a function of relative humidity for $\text{CaCO}_3(1\ 0\ 4)$, before and after reaction with nitric acid vapor at 23% RH. The number of water layers taken up by the surface is determined from FTIR spectroscopy by using the integrated absorbance of the water absorption band near $3400\ \text{cm}^{-1}$. The surface density of adsorbed water, $S(\text{H}_2\text{O})$ in molecule/ cm^2 , is related to the integrated absorbance of the O—H band according to [44,50],

$$S(\text{H}_2\text{O}) = \frac{2.303\tilde{A}(\text{OH})\cos\phi}{N\bar{\sigma}} \quad (4)$$

where $\tilde{A}(\text{OH})$ is the integrated absorbance of the O—H band (cm^{-1}), N is the number of adsorption surface faces

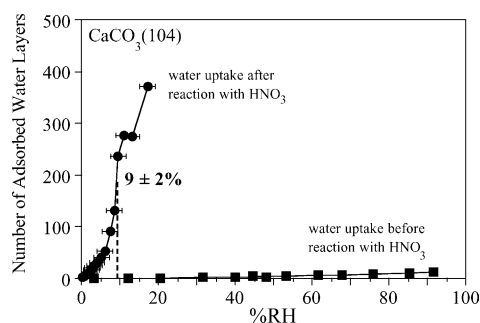


Fig. 10. The number of adsorbed water layers on $\text{CaCO}_3(1\ 0\ 4)$, before and after reaction with nitric acid vapor at 23% RH is plotted as a function of relative humidity. There is clearly an increase in the hygroscopic response of these surfaces after reaction with nitric acid, which is attributed to the deliquescence of the $\text{Ca}(\text{NO}_3)_2$ product at $9 \pm 2\%$. Adapted with permission from H.A. Al-Abadleh, B.J. Krueger, J.L. Ross, V.H. Grassian, Phase transitions in calcium nitrate thin films, Chem. Commun. (2003) 2796. Copyright (2003) The Royal Society of Chemistry.

(6 in these experiments), σ is the integrated cross section of O—H band of liquid water and has a value of $1.07 \times 10^{-16}\ \text{cm molecule}^{-1}$ [51], and ϕ is the angle of incidence, 45° . The number of adsorbed water layers can be calculated by normalizing $S(\text{H}_2\text{O})$ values to the surface density of the hydroxylated calcite surface, which is for an unreconstructed surface estimated to be $1 \times 10^{15}\ \text{mol cm}^{-2}$ for water [52].

From thermodynamic considerations, it is expected that $\text{Ca}(\text{NO}_3)_2$ will be converted to $\text{Ca}(\text{NO}_3)_2 \cdot 4\text{H}_2\text{O}$ at 11.8% RH [53]. From solution phase thermodynamics, the DRH should occur at the RH humidity of a saturated solution, i.e., to say the DRH is equal to the water activity, $p/p_0 \times 100$, where p_0 is the vapor pressure above pure water and p is the water vapor pressure above the solution. In agreement with earlier measurements [54], we have measured the vapor pressure above a saturated water solution of calcium nitrate to be $57 \pm 5\%$ RH at room temperature. Thus, the crystalline tetrahydrate phase is expected to deliquesce at 57% RH. Instead, a DRH near 10% is measured for calcium nitrate thin films supported on calcium carbonate. A possible reason for the discrepancy between the measured DRH and that predicted from thermodynamics is due to the fact that calcium nitrate forms a metastable amorphous layer that undergoes deliquescence instead of crystallization to the stable tetrahydrate phase at low relative humidity.

4. Conclusions

Clearly water plays an important role in the composition and reactivity of oxide and carbonate surfaces under environmental conditions. For MgO and CaCO_3 , it has been shown from a variety of studies and experimental data that these surfaces are truncated with hydroxyl groups and adsorbed water in the presence of water vapor. The reactivity of MgO and CaCO_3 toward nitric acid increases in the presence of adsorbed water on the surface. This increase in reactivity may be related to an increase in the ionic mobility on the wetted surface allowing for further reaction to occur with underlying layers. The nitric acid reacted MgO and CaCO_3 surfaces show several phase transitions as a function of increasing and decreasing relative humidity. Phase transitions in these thin nitrate films of $\text{Mg}(\text{NO}_3)_2$ and $\text{Ca}(\text{NO}_3)_2$ differ from that predicted from bulk phase thermodynamics. This discrepancy is most likely due to the formation of metastable amorphous layers in these thin films. A further understanding of metastable phases of salts is warranted if these non-equilibrium phases form under ambient conditions of temperature and relative humidity [55,56].

Acknowledgement

The authors greatly appreciate the support of the National Science Foundation through a creativity extension of CHE-9984344.

References

- [1] H.H. Kung, *Transition Metal Oxides: Surface Chemistry and Catalysis*, Vol.45, Elsevier, Amsterdam, 1989.
- [2] V.E. Henrich, P.A. Cox, *Appl. Surf. Sci.* 72 (1993) 277.
- [3] M. Blesa, P. Moran do, A. Reason, *Chemical Dissolution of Metal Oxides*, CRC Press, Florida, 1993.
- [4] W. Stem, *Chemistry of the Solid-Water Interface*, John Wiley and Sons, New York, 1992.
- [5] P.J. Eng, T.P. Trainer, G.E. Brown Jr., G.A. Waychunas, M. Newville, S.R. Sutton, M.L. Rivers, *Science* 288 (2000) 1029.
- [6] K.C. Hass, W.F. Schneider, A. Curioni, W. Andreoni, *J. Phys. Chem. B* 104 (2000) 5527, and references within.
- [7] J.W. Elam, C.E. Nelson, M.A. Cameron, M.A. Tolbert, S.M. George, *J. Phys. Chem. B* 102 (1998) 7008.
- [8] P. Liu, T. Kendelewicz Jr., G.E. Brown, G.A. Parks, *Surf. Sci.* 412/413 (1998) 287.
- [9] P. Liu, T. Kendelewicz Jr., G.E. Brown, G.A. Parks, *Surf. Sci.* 412/413 (1998) 315.
- [10] R.W.G. Wyckoff, 2nd ed., *Crystal Structures*, Vol.2, Interscience Publishers, New York, 1963.
- [11] N.H. de Leeuw, S.C. Parker, *J. Phys. Chem. B* 102 (1998) 2914.
- [12] S.A. Chambers, *Surf. Sci. Rep.* 39 (2000) 105.
- [13] D.W. Goodman, *J. Vac. Sci. Technol. A* 14 (1996) 1526.
- [14] C. Duriez, C. Chapon, C.R. Henry, J.M. Rickard, *Surf. Sci.* 230 (1990) 123.
- [15] G.A. Somorjai, *Introduction to Surface Chemistry and Catalysis*, John Wiley & Son, Inc., New York, 1994.
- [16] M.I. McCarthy, G.K. Schenter, C.A. Scamehorn, J.B. Nicholas, *J. Phys. Chem.* 100 (1996) 16989.
- [17] M.A. Johnson, E.V. Stefanovich, T.N. Truong, *J. Phys. Chem. B* 102 (1998) 6391.
- [18] C.A. Scamehorn, N.M. Harrison, M.I. McCarthy, *J. Chem. Phys.* 101 (1994) 1547.
- [19] C.A. Scamehorn, A.C. Hess, M.I. McCarthy, *J. Chem. Phys.* 99 (1993) 2786.
- [20] M. Odelius, *Phys. Rev. Lett.* 82 (1999) 3919.
- [21] J.-H. Cho, J.M. Park, K.S. Kim, *Phys. Rev. B* 62 (2000) 9981.
- [22] O. Engkvist, A.J. Stone, *Surf. Sci.* 437 (1999) 239.
- [23] D. Abriou, J. Jupille, *Surf. Sci.* 430 (1999) L527.
- [24] M.A. Johnson, E.V. Stefanovich, T.N. Truong, J. Günster, D.W. Goodman, *J. Phys. Chem. B* 103 (1999) 3391.
- [25] C. Xu, D.W. Goodman, *Chem. Phys. Lett.* 265 (1997) 341.
- [26] C.-M. Wu, C.A. Estrada, J.S. Corneille, D.W. Goodman, *J. Chem. Phys.* 96 (1992) 3892.
- [27] J. Heidberg, B. Redlich, D. Wetter, *Ber. Bunsenges. Phys. Chem.* 99 (1995) 1333.
- [28] J. Günster, G. Liu, J. Stultz, S. Krischok, D.W. Goodman, *J. Phys. Chem. B* 104 (2000) 5738.
- [29] D. Ferry, A. Glebov, V. Senz, J. Suzanne, J.P. Toennies, H. Weiss, *Surf. Sci.* 337/379 (1997) 634.
- [30] H.J. Kim, J. Kang, M.Y. Song, S.H. Park, D.G. Park, H.J. Kweon, S.S. Nam, *Bull. Korean Chem. Soc.* 20 (1999) 786.
- [31] S. Coluccia, S. Lavagnino, L. Marchese, *Mater. Chem. Phys.* 18 (1988) 445.
- [32] M.R. Carrott, P. Carrott, M.B. de Carvalho, K.S.W. Sing, *J. Chem. Soc. Faraday Trans.* 89 (1993) 579.
- [33] M. Foster, M. Furse, D. Passno, *Surf. Sci.* 502–503 (2002) 102.
- [34] H.D. Kim, R.M. Lynden-Bell, A. Alavi, J. Stultz, D.W. Goodman, *Chem. Phys. Lett.* 352 (2002) 318.
- [35] P.A. Campbell, *Inst. Phys. Conf. Ser.* 168–11 (2001) 513.
- [36] S.L.S. Stipp, C.M. Eggleston, B.S. Nielsen, *Geochim. Cosmochim. Acta* 58 (1994) 3023.
- [37] S.L.S. Stipp, W. Gutmannsbauer, T. Lehmann, *Am. Mineral.* 81 (1996) 1.
- [38] S.L.S. Stipp, *Geochim. Cosmochim. Acta* 63 (1999) 3121.
- [39] S.I. Kuriyavar, R. Vetrivel, S.G. Hegde, A.V. Ramaswamy, D. Chakraborty, S. Mahapatra, *J. Mater. Chem.* 10 (2000) 1835.
- [40] E. Stöckelmann, R. Hentschke, *Langmuir* 15 (1999) 5141.
- [41] J.M. McCoy, J.P. LaFemina, *Surf. Sci.* 373 (1997) 288.
- [42] S.L.S. Stipp, M.F. Hochella, *Geochim. Cosmochim. Acta* 55 (1991) 1723.
- [43] H.A. Al-Hosney, V.H. Grassian, unpublished results.
- [44] W. Cantrell, G.E. Ewing, *J. Phys. Chem. B* 105 (2001) 5434.
- [45] V. Sadtschenko, P. Conrad, G.E. Ewing, *J. Chem. Phys.* 116 (2002) 4293.
- [46] H.A. Al-Abadleh, V.H. Grassian, *J. Phys. Chem. B* 107 (2003) 10829.
- [47] A.L. Goodman, G.M. Underwood, V.H. Grassian, *J. Geophys. Res. Atmos.* 104 (2000) 29053.
- [48] H.A. Al-Hosney, V.H. Grassian, *J. Am. Chem. Soc.* 126 (2004) 8068.
- [49] H.A. Al-Abadeh, B.J. Krueger, J.L. Ross, V.H. Grassian, *Chem. Commun.* (2003) 2796.
- [50] H.A. Al-Abadleh, V.H. Grassian, *Langmuir* 19 (2003) 341.
- [51] H.D. Downing, D.J. Williams, *J. Geophys. Res.* 80 (1975) 1656.
- [52] H.A. Al-Abadleh, Ph.D. Dissertation, University of Iowa, 2003.
- [53] I.N. Tang, K.H. Fung, *J. Chem. Phys.* 106 (1997) 1653.
- [54] F. Pique, L. Dei, E. Ferroni, *Stud. Conserv.* 37 (1992) 217.
- [55] I.N. Tang, K.H. Fung, D.G. Imre, H.R. Munkelwitz, *Aerosol Sci. Technol.* 23 (1995) 443.
- [56] A.S. Ansari, S.N. Pandis, *Atmos. Env.* 34 (2000) 157.